

Supplementary information for

Nanomolar LL-37 induces permeability of a biomimetic mitochondrial membrane

Xin Jiang[†], Chenguang Yang[†], Jie Qiu, Dongfei Ma, Cheng Xu, Shuxin Hu, Weijing

Han^{*}, Bing Yuan^{*}, and Ying Lu^{*}

X. Jiang[†], J. Qiu, D. Ma, C. Xu, W. Han^{*}, B. Yuan^{*}

Songshan Lake Materials Laboratory, Dongguan, Guangdong 523808, China

C. Yang[†], S. Hu, Y. Lu^{*}

Beijing National Laboratory for Condensed Matter Physics, Institute of Physics,
Chinese Academy of Sciences, Beijing 100190, China; University of Chinese
Academy of Sciences, Beijing 100049, China

C. Xu

Center for Soft Condensed Matter Physics and Interdisciplinary Research & School of
Physical Science and Technology, Soochow University, Suzhou, Jiangsu 215006,
China

[†]These authors contributed equally to this work.

*E-mails: hanweijing@sslabor.org.cn (W. Han); yuanbing@sslabor.org.cn (B. Yuan);
yinglu@iphy.ac.cn (Y. Lu)

Materials and methods

Supplementary images (Figure S1-S14) and corresponding notes

Supplementary tables (Table S1-S3)

Materials and methods

Materials

1,2-dioleoyl-sn-glycero-3-phosphocholine (DOPC), 1,2-dioleoyl-sn-glycero-3-phosphate (DOPA), 1,2-dioleoyl-sn-glycero-3-phosphoethanolamine (DOPE), 1,2-dioleoyl-sn-glycero-3-phospho-(1'-rac-glycerol) (DOPG), 1,2-dipalmitoyl-sn-glycero-3-phosphoethanolamine-N-(capbiotinyl) (Biotinyl-cap PE) and 1,2-dioleoyl-sn-glycero-3-phosphoethanolamine-N-(Cyanine 5) (Cy5 PE) were purchased from Avanti Polar Lipids (Alabaster, AL, USA). Fluo-4 fluorophore was from Thermofisher. DNase I and Bovine albumin (BSA) were from Sigma-Aldrich. Lysozyme and streptavidin were from BBI. The unlabeled LL-37 and carboxy-tetramethylrhodamine (TAMRA) labeled LL-37 were synthesized by China Peptides Co. Ltd.

Preparation of the model membrane systems

Three types of model membrane systems were fabricated, including a PE-rich membrane, DOPE/DOPG = 90/10 (by mol), mimicking the mitochondrial outer membranes,^{1, 2} a PC-rich membrane, DOPC/DOPG = 90/10 (by mol), mimicking the eukaryotic plasma membranes,³ and a heavily negatively charged PA-rich membrane, DOPA/DOPG = 90/10 (by mol).

The lipids were dissolved in chloroform at 10 mg/mL and mixed at certain molar ratios as mentioned above. The mixed lipid solution was dried under nitrogen flow, and evaporated in vacuum for at least 2 h to form a thin lipid film. Potassium dihydrogen phosphate-sodium dihydrogen phosphate buffer (phosphate buffer) was added (final lipid concentration is 2 mg/mL) and shaken for 1 h to resuspend the lipids. The solution was ultrasonicated until the liquid turned clear to form liposomes. The liposome dispersion was forced to go through a polycarbonate filter with 100 nm pore size (GE Healthcare) using a mini-extruder (Avanti Polar Lipids) to form homogenous unilamellar vesicles for the following leakage or imaging experiments.

Circular dichroism (CD) spectroscopy measurement

Solution containing 5 μ M LL-37 peptide was used in the CD experiment to get the spectrum in buffer. To obtain the spectrum in membrane, LL-37 was added to liposomes with varying lipid compositions at 1:100 (by mol). The CD spectroscopy was performed on a J-715 spectropolarimeter (Jasco) using a 2 mm pathlength quartz cell, and the data was collected in continuous scanning mode between 190 and 260 nm. All displayed CD spectra were the accumulation of at least three scans. The helical content (percentage of helix) was estimated from the molar ellipticity at 222 nm.

Liposome leakage assay

For the liposomes used in the vesicle leakage assay, the lipids were premixed with Biotinyl cap PE (0.1 mol%) and Cy5-PE (0.002 mol%), and phosphate buffer containing Fluo-4 (at 25 μ g/mL) was added to the lipid film for lipid rehydration to form Fluo-4 encapsulated liposomes.

The liposomes were immobilized on the substrate surface via biotin-streptavidin interaction. A coverslip was coated with polyethylene glycol (mPEG-SVA and Biotin-PEG-SVA, 99:1 molar ratio),⁴ and assembled into a home-made flow chamber. Phosphate buffer containing streptavidin (at 0.01 mg/mL) was flowed in and incubated for 10 min at the room temperature. After that, the Fluo-4-encapsulated liposomes were added and incubated for 5 min, followed by a gentle washing to remove the excessive vesicles. The system was observed under fluorescence microscope. Phosphate buffer containing Ca^{2+} (at 10 μ M) and LL-37 (at certain concentrations as detailed in the main text) was added in situ at the time point of 0 min, and images were taken in both the Fluo-4 (ex 488 nm, em 585 nm \pm 32.5 nm) and Cy5 (ex 640 nm, em 697 nm \pm 30 nm) channels with a 50 ms time resolution.

Ca^{2+} could rise the fluorescent quantum yield of Fluo-4,⁵ thus the fluorescence intensity of Fluo-4-encapsulated liposome increases when the transmembrane Ca^{2+} influx occurs due to peptide-induced permeabilization of the membrane. Based on the

TIRFM images, the ratio between the counts of visible liposomes in the Fluo-4 channel, representing the number of permeabilized liposomes, and the counts of liposomes in the Cy5 channel, representing the total number of liposomes under observation, was recorded over time to demonstrate the LL-37-induced permeabilization of membranes. The images were recorded over time, then the percentage of the permeabilized liposomes was calculated.

Single-molecule fluorescent imaging and quantitative analysis

Supported lipid bilayers (SLBs) with varying lipid compositions were prepared via vesicle fusion. The liposome dispersion was flowed into a home-made chamber cell with a pre-cleaned cover-slip substrate, incubated at 37 °C overnight, and washed gently with phosphate buffer to remove the excessive vesicles. The system was observed under TIRF microscope. 1 nM TAMRA-labeled LL-37 solution was added to different membrane systems as stated in the main text at the time point of 0 min, and time-lapse images were recorded at different time points.

To compare the accumulation state of LL-37 in different lipids, the mean amount of fluorescent peptides in the field of vision, N , was calculated and compared among different membrane systems. At each time point, five frames (50 ms/frame) were acquired for average; after that, the whole view was photobleached and another five frames were acquired for average as the background. The total brightness of these two averaged frames was recorded as I and I_{Back} , respectively, using ImageJ software. Based on this, the net intensity of the fluorescent peptides at this time point (of the 256×256 pixels, $40 \times 40 \mu\text{m}$ area) could be obtained as $F = (I - I_{Back})$. On the other hand, the net intensity of a single fluorescent peptide was calculated as $F' = (I' - I'_{Back})$, in which I' referred to the fluorescent intensity of a single fluorophore with a selection area of 7×7 pixels and I'_{Back} is the fluorescent intensity in another 7×7 pixels area without fluorophore. Therefore, the value of N could be calculated as

$$N = \frac{F}{F'} = \frac{I - I_{Back}}{I' - I'_{Back}} \quad (1)$$

To determine the oligomerization level of LL-37, another parameter of n , referring to the number of molecules accumulated in an individual oligomer, was calculated.^{6,7} Intensity traces over time of individual fluorescent spots were derived from the movies by ImageJ software and statistics were carried out by the scripts written in MATLAB (Mathworks). For steady intensity traces, the difference of the intensity before and after photobleaching represented the intensity of the molecule. The value of n was determined based on the single-molecule stepwise photobleaching of dye molecules in the spot. The unbiased step-finding algorithm⁸ was applied to determine the intensity and length of the steps.

Z-position determination of individual peptides

A surface-induced fluorescence attenuation (SIFA) test was performed to determine the Z position of individual molecules in real time.⁹ Before SLB deposition, the coverslip substrate was pre-deposited with a monolayer of graphene oxide (GO) synthesized following the modified Hummers method,⁹ using the traditional Langmuir-Blodgett deposition method. 1 mM BSA in phosphate buffer was added to incubate the GO-coated substrate for 30 min, and washed gently with buffer. Then, liposomes with certain lipid compositions were added and incubated at 37 °C overnight for the formation of a planar lipid bilayer. The GO and BSA layer worked as fluorescent receptor and spacer, respectively, in the SIFA test. The peptide-membrane interaction process was also monitored under TIRFM (in the TAMRA channel), and time evolution of the fluorescence intensity of each spot was analyzed by ImageJ.

The SIFA method provides a quantitative correlation between fluorescence intensity and Z position of the fluorophore (i.e., the distance of probe from GO surface), following

$$\frac{F}{F_0} = \frac{(d/d_0)^4}{[1+(d/d_0)^4]} \quad (2)$$

where F and F_0 refer to the fluorescence intensity of individual probe on the substrate regions with and without GO, respectively. d refers to Z position of the probe. d_0 is the characteristic quenching distance at which $F/F_0 = 1/2$, which was determined to be 4.3 nm.⁹ Based on this, time evolution of Z position of the TAMRA-labeled peptide was given under different experimental conditions. The traces showing intensity changes represented multiple dynamic processes of the LL-37.

***Escherichia coli* protoplasts assay**

The *E. coli* protoplasts were prepared following a previous protocol.¹⁰ *E. coli* K12 was grown in LB broth overnight and placed in 10 mL LB broth for 2 hours until the OD600 value turned to ~0.6. The cells were centrifuged at room temperature 4000 rpm, for 10 min (LEGEND MICRO 21R, Thermo scientific). After that, the pellet was resuspended in 10 mL SP buffer with 10 U/mL DNase I and 50 µg/mL lysozyme. The mixture was incubated at 30 °C for 20 min to destroy the cell wall and form cell protoplasts. The cell protoplasts were centrifuged at room temperature 4000 rpm for 5 min, and the pellet was resuspended in M9 medium. Then, the mixture was diluted 1000 times by M9 medium with 1 µg/mL ampicillin and 10 U/mL DNase I.

The protoplasts were observed under an objective-based total internal reflection fluorescence microscope (TIRFM; Ti2, Nikon) equipped with an EMCCD camera (DU-897, Andor). TAMRA-labeled LL-37 (to a final concentration of 10 nM) and PI solution (to a final concentration of 1 µg/mL) was added to check the permeabilization of the membrane. The Pseudo-TIRF was adopted in the *E. coli* cells protoplasts imaging. Images were taken in the transmission, TAMRA (ex 532 nm, em 585 nm±32.5 nm) and PI (ex 532 nm, em 697 nm±30 nm) channels. For comparison, the protoplasts without peptide addition were also observed.

Supplementary Images

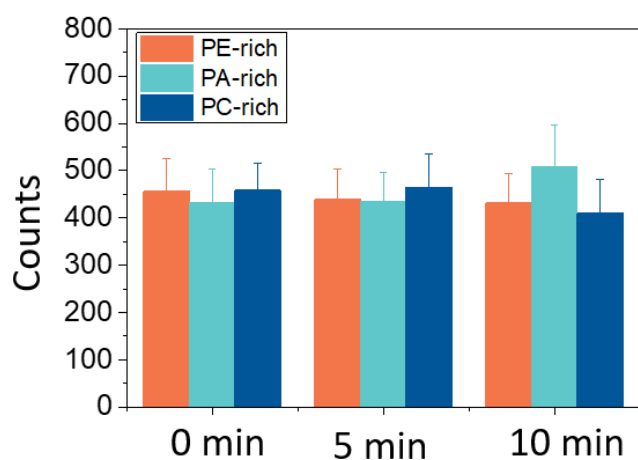


Figure S1. Time evolution of the number of liposomes immobilized on the substrate in the vesicle leakage assay. The liposomes are composed of different lipid species as marked in the graph.

Corresponding notes

There is no significant change in the number with time showing stability of the liposome system under observation.

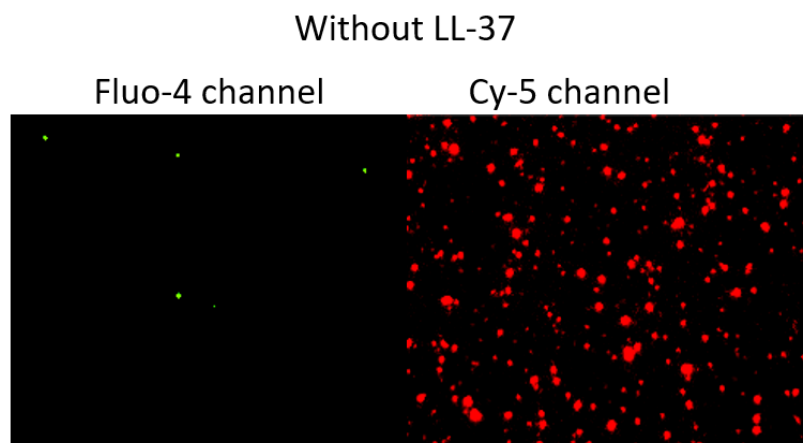


Figure S2. Representative fluorescent image of the PE-rich liposomes after 10 min incubation with Ca^{2+} -containing buffer (without LL-37 addition) under observation. The liposomes were labeled with Cy5-PE, and encapsulated with Fluo-4.

Corresponding notes

No distinguishable fluorescence is observed in the Fluo-4 channel, indicating no transmembrane entry of Ca^{2+} in the system without LL-37 addition.

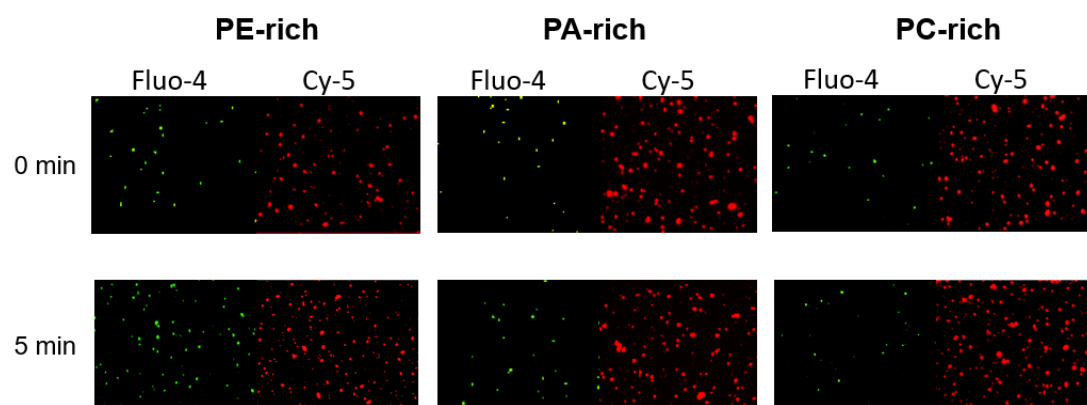


Figure S3. Representative fluorescent images of the liposomes, composed of different lipid species, 0 or 5 min after LL-37 addition. The liposomes are labeled with Cy5-PE, encapsulated with Fluo-4, and surrounded with Ca^{2+} -containing buffer. LL-37 is added at the time of 0 min.

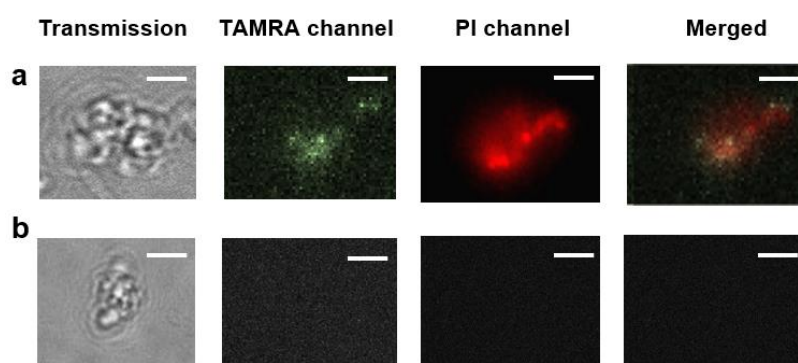


Figure S4. Membrane permeabilizing effect of LL-37 over the *E. coli* protoplasts. (a, b) The phase contrast and fluorescent images (in 532 nm TAMRA emission channel and 640 nm PI emission channel) of the *E. coli* protoplasts with 10 nM TAMRA-labeled LL-37 and 1 $\mu\text{g}/\text{mL}$ PI (a), or with 1 $\mu\text{g}/\text{mL}$ PI but without TAMRA-labeled LL-37 (b). Scale bar in the image is 3 μm .

Corresponding notes

To test the membrane permeabilizing ability of LL-37 over bacterial membranes, the *E. coli* protoplasts were exposed to TAMRA-labeled LL-37 (10 nM) with the membrane impermeant DNA dye PI (1 $\mu\text{g}/\text{mL}$). The fluorescence of PI is enhanced about 30-fold when bound to nucleic acids.

After 10 minutes incubation, fluorescence on the protoplast's membrane in the TAMRA channel represents the membrane-association of LL-37. The co-localized fluorescence in the PI channel indicates LL-37 destroys *E. coli* membrane and PI gets into the cytoplasm. As negative control, the protoplasts with PI but without the

addition of LL-37 show that there is no fluorescence in either the TAMRA or the PI channel. This suggests the protoplasts remain integrity in PI solution.

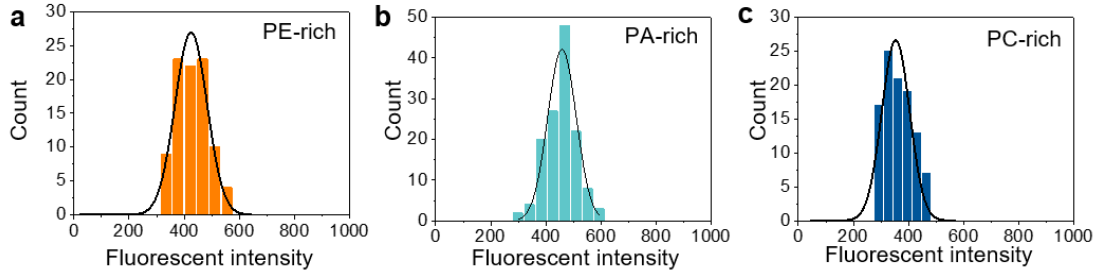


Figure S5. Determination of the pristine fluorescence intensity value, F_0 , of TAMRA-labeled LL-37, on a PE- (a), PA- (b) or PC-rich membrane (c). For each graph, 150-200 traces were used.

Corresponding notes

For accuracy, the value of F_0 was determined respectively for the PE-, PA- and PC-rich bilayers. Such deviations in F_0 values might be ascribed to the influence of probe environment.

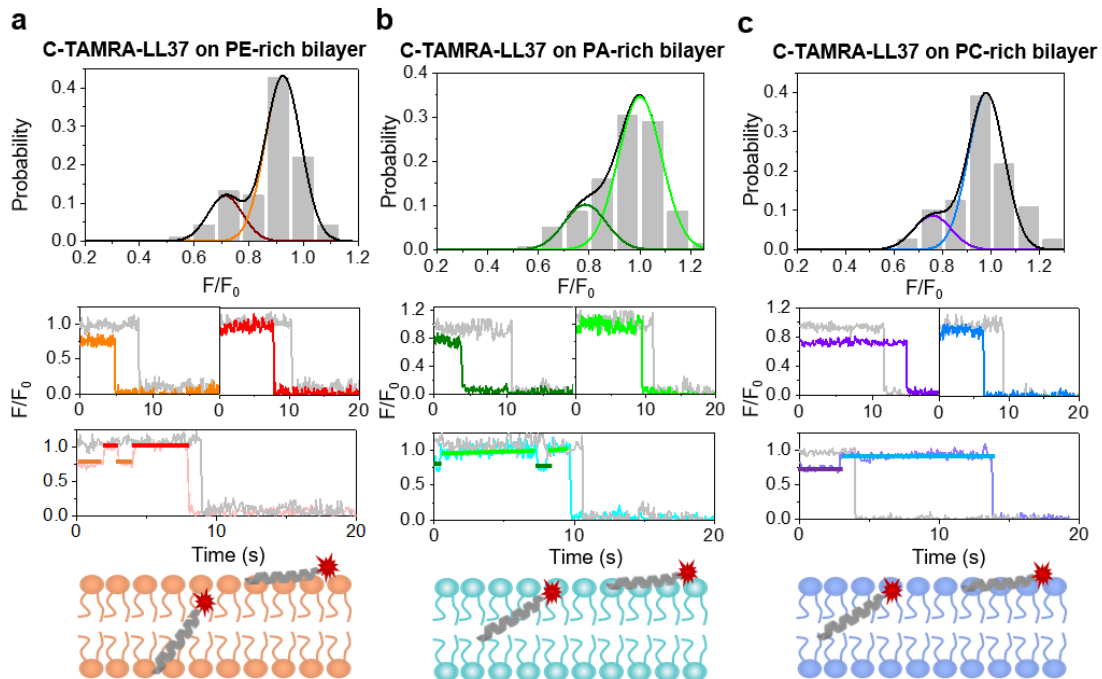


Figure S6. Insertion-depth determination of C-termini of the C-TAMRA-LL-37 in

different lipid bilayers, i.e., PE- (a), PA- (b) and PC-rich SLB (c). Top graph, fluorescence intensity distributions analyzed based on more than 100 traces each. Colored lines show fitting curves and determination of states. Middle, representative fluorescence intensity traces (after normalization) of peptides. Colored straight lines are step fits of the traces. Reference molecules (on the substrate region without GO) are also shown (in grey). Bottom, configurational cartoons showing the mean position of fluorescence-labeled C-terminal corresponding to each state in the membrane. The data were collected immediately after LL-37 addition.

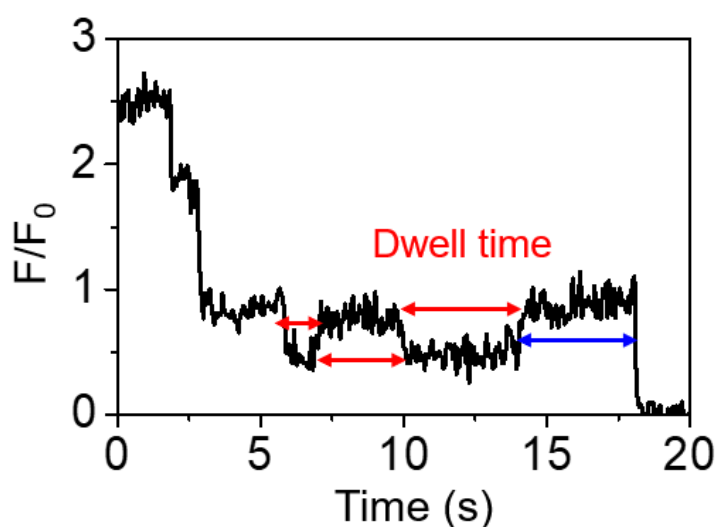


Figure S7. Definition of dwell time in the SIFA experiment. The definition of the dwell time is indicated by a red line. In order to avoid the influence of photobleaching on the statistics of dwell time, the last states (blue line) are not included in dwell time statistics.

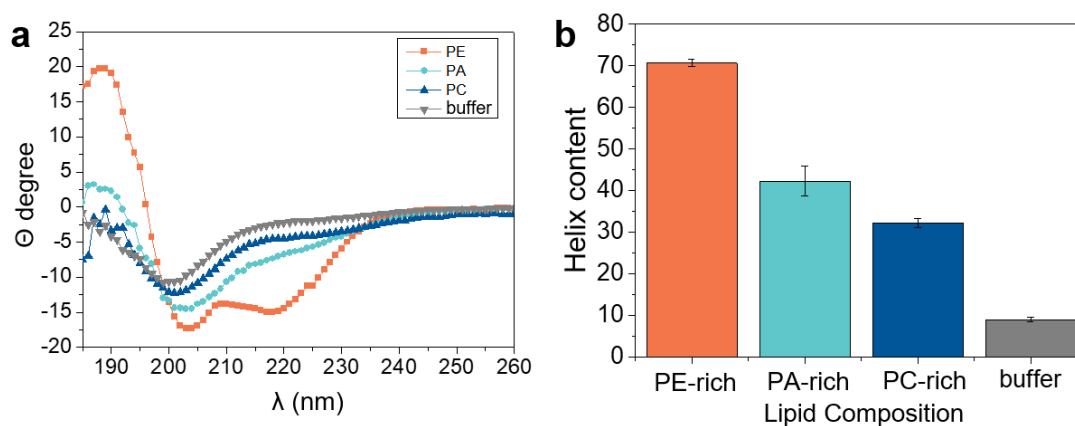


Figure S8. CD spectra and corresponding helical contents of LL-37 in PE-, PA-, and PC-rich liposome dispersions and in buffer. The statistics in (b) correspond to at least three independent

experiments, and the error bars represent the statistical error.

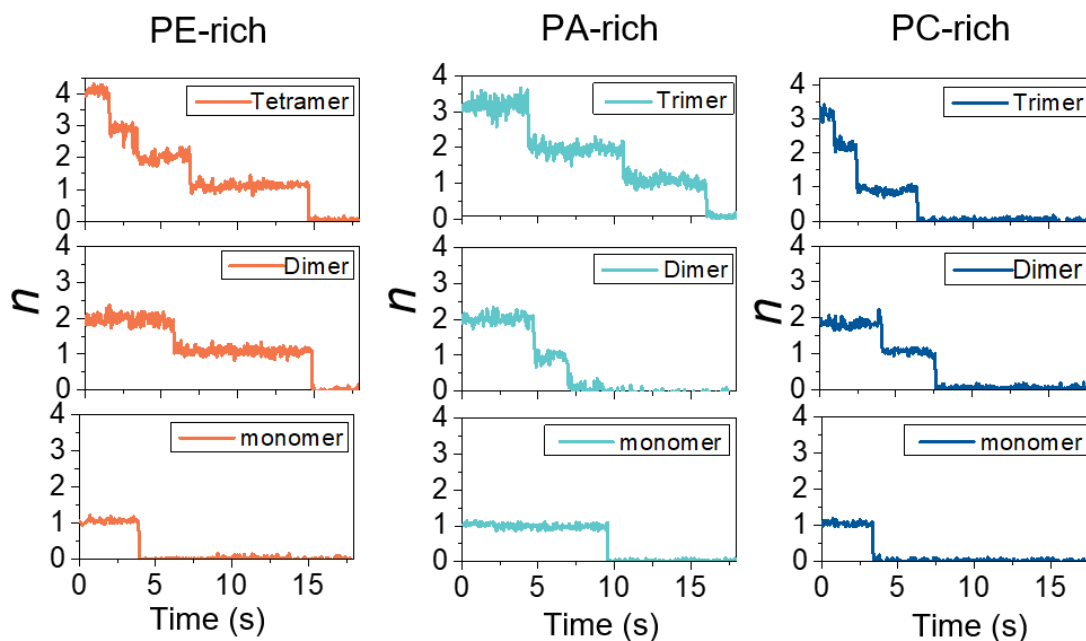


Figure S9. Representative intensity traces and determination of oligomerization level (n) of TAMRA-labeled LL-37 on/in different membranes. The steps referring to photobleaching of individual fluorophores within each spot.

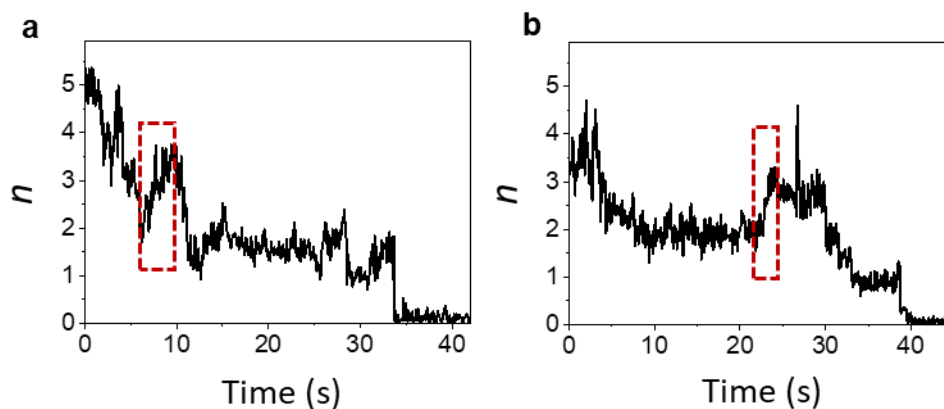


Figure S10. Representative traces of individual LL-37 oligomers on/in a PE-rich membrane. The rising stages of the curve, marked with dotted red rectangles, probably refer to the “aggregation/oligomerization” process.

Percentage of liposomes with green fluorescence

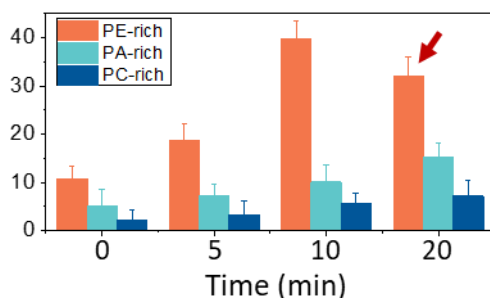


Figure S11. Percentage of liposomes with green fluorescence after the addition of LL-37. The statistics correspond to at least three independent experiments, and the error bars represent the statistical error. The liposomes were labeled with Cy5-PE (red color), encapsulated with Fluo-4, and dispersed in a solution containing 10 mM Ca^{2+} . Label-free LL-37 was added at the time of 0 min with a final concentration of 10 nM. The entry of Ca^{2+} into liposomes due to peptide-induced permeabilization of the membrane could enhance the Fluo-4 fluorescence signal (green color), which could be observed in situ under TIRFM.

As shown in Figure S11, the percentage of liposomes with green fluorescence increases with time after the addition of LL-37, especially for the PE-rich system. This indicates the peptide-induced permeabilization of membranes and entry of Ca^{2+} . However, at the time of 20 min, the percentage of fluorescent liposomes decreases in the PE system (marked with red arrow). This indicates the leakage of Fluo-4 from the interior of liposomes to the outside, suggesting the formation of larger transmembrane defects (e.g., pores) due to peptide actions.

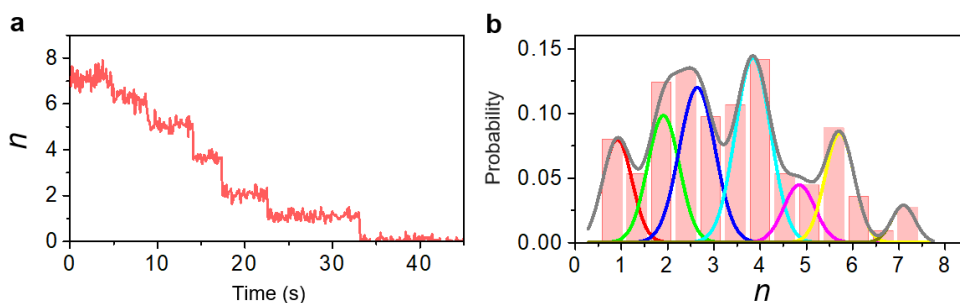


Figure S12. Representative intensity trace and determination of oligomerization level (n) of TAMRA-labeled LL-37 on/in the *E. coli* protoplast membrane. (a) Intensity trace. The steps referring to photobleaching of individual fluorophores within the oligomer. (b) Histograms showing distribution of n . The data was based on 3 independent experiments.

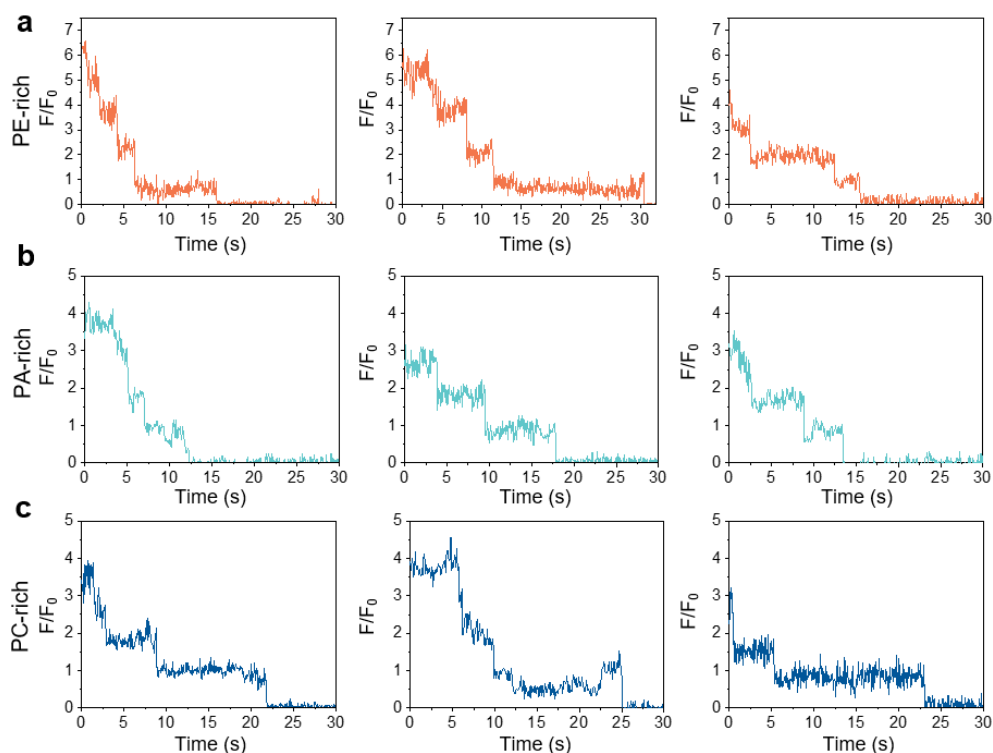


Figure S13. Typical fluorescence traces of oligomerized LL-37 in SIFA tests. (a), (b) and (c) refer to the PE-, PA- and PC-rich SLBs, respectively. The SLBs were incubated with 1 nM N-TAMRA-LL-37 for 120 min before trace selection.

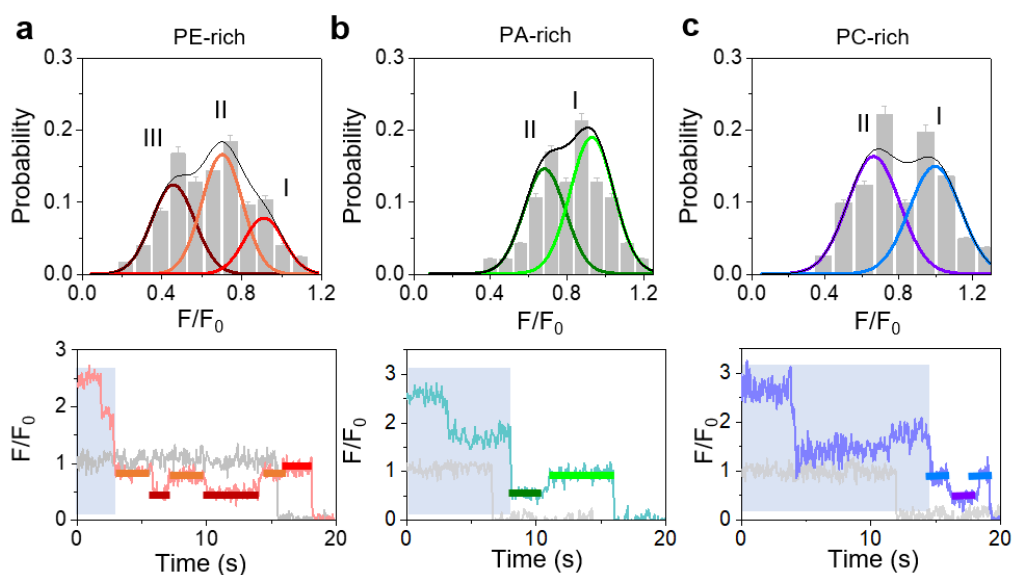


Figure S14. Insertion states of LL-37 trimers in different lipid bilayers, i.e., the PE- (a), PA- (b) or PC-rich (c) bilayers. Top graph, fluorescence intensity distributions of the LL-37s fluorescent intensity. Colored lines show fitting curves and determination of states. Bottom, representative fluorescence intensity trace (after normalization) of

peptides. The last stage (referring to single molecular fluorescence) is selected for analysis and colored straight lines are step fits. A reference molecule (on the substrate region without GO) is also shown (in grey). The SLBs were incubated with 1 nM N-TAMRA-LL-37 for 120 min before trace selection.

Supplementary Tables

Table S1. Insertion state of N-TAMRA-LL-37 in a PE-rich bilayer, as monomers, dimers, or tetramers.

		State I	State II	State III
Monomer¹	F/F_0	90%±10%	73%±10%	42%±10%
	Z-position ²	4.0±1.3 nm	2.0±0.7 nm	0.3±0.4 nm
	proportion	36.6%	46.2%	15.8%
Dimer¹	F/F_0	91%±11%	71%±11%	38%±11%
	Z-position	4.3 nm±1.3 nm	2.3 nm±0.7 nm	0.3 nm±0.4 nm
	proportion	36.1%	47.4%	16.5%
Tetramer¹	F/F_0	89%±16%	75%±16%	39%±16%
	Z-position	3.9 nm±1.7 nm	2.4 nm±0.9 nm	0.3 nm±0.5nm
	proportion	20.2%	37.4%	42.3%

¹The data of monomers were collected immediately after peptide addition, while that of dimers and tetramers were collected after 120 min peptide incubation (at 1 nM).

²Z-position refers to the distance of the probe from the bottom of the bilayer.

Table S2. Insertion state of N-TAMRA-LL-37 in a PA-rich bilayer, as monomers, dimers, or tetramers.

		State I	State II (II'/II'')	State III
Monomer	F/F_0	90%±9%	78%±9% 63%±9%	
	Z-position	4.1 nm±1.2 nm	2.6 nm±0.8 nm 1.8 nm±0.6 nm	
	proportion	62%	23% 15%	
Dimer	F/F_0	90%±13%	68%±13%	
	Z-position	4.1 nm±1.5 nm	2.0±0.7 nm	
	proportion	52%	48%	
Tetramer	F/F_0	89%±12%	77%±12%	39%±12%

	Z-position	3.9 nm±1.5 nm	2.6 nm±0.7 nm	0.3 nm±0.4 nm
	proportion	30.4%	40.2%	29.4%

Table S3. Insertion state of N-TAMRA-LL-37 in a PC-rich bilayer, as monomers, dimers, or tetramers.

		State I	State II	State III
Monomer	F/F_0	89%±9%	70%±9%	
	Z-position	4.2±1.4 nm	1.8±0.6 nm	
	proportion	88.5%	21.5%	
Dimer	F/F_0	90%±14%	67%±14%	
	Z-position	4.1 nm±1.6 nm	2.0±0.7 nm	
	proportion	42%	58%	
Tetramer	F/F_0	92%±11%	68%±11%	41%±11%
	Z-position	4.6 nm±1.4 nm	2.3 nm±0.7 nm	0.4 nm±0.4 nm
	proportion	35.6%	38.9%	24.6%

Reference

1. E. Zinser, C. D. M. Sperka-Gottlieb, E.-V. Fasch, S. D. Kohlwein, F. Paltauf and G. Daum, *J. Bacter.*, 1991, **173**, 2026-2034.
2. D. Patel and S. N. Witt, *Oxid. Med. Cell. Longev.*, 2017, **2017**, 4829180.
3. M. R. Sanders, L. A. Clifton, R. A. Frazier and R. J. Green, *Langmuir*, 2017, **33**, 4847-4853.
4. C. Joo, S. A. McKinney, M. Nakamura, I. Rasnik, S. Myong and T. Ha, *Cell*, 2006, **126**, 515-527.
5. N. Bondre, Y. X. Zhang and C. D. Geddes, *Sensor. Actuat. B-Chem.*, 2011, **152**, 82-87.
6. J. Xu, G. Qin, F. Luo, L. Wang, R. Zhao, N. Li, J. Yuan and X. Fang, *J Am Chem Soc*, 2019, **141**, 6976-6985.
7. L. Dresser, P. Hunter, F. Yendybayeva, A. L. Hargreaves, J. A. L. Howard, G. J. O. Evans, M. C. Leake and S. D. Quinn, *Methods*, 2021, **193**, 80-95.
8. J. W. J. Kerssemakers, E. Laura Munteanu, L. Laan, T. L. Noetzel, M. E. Janson and M. Dogterom, *Nature*, 2006, **442**, 709-712.
9. Y. Li, Z. Qian, L. Ma, S. Hu, D. Nong, C. Xu, F. Ye, Y. Lu, G. Wei and M. Li, *Nat. Commun.*, 2016, **7**, 12906.
10. T. Kuroda, N. Okuda, N. Saitoh, T. Hiyama, Y. Terasaki, H. Anazawa, A. Hirata, T. Mogi, I. Kusaka, T. Tsuchiya and I. Yabe, *J Biol Chem*, 1998, **273**, 16897-16904.